Observation of the $Y(4230)$ and evidence for a new vector charmonium-like state $Y(4710)$ in $e^+e^- \to K_S^0 K_S^0 J/\psi$

M. Ablikim[1], M. N. Achasov[11,b], P. Adlarson[70], M. Albrecht[4], R. Aliberti[31], A. Amoroso[69A,69C], M. R. An[35], Q. An[66,53], X. H. Bai[61], Y. Bai[52], O. Bakina[32], R. Baldini Ferroli[26A], I. Balossino[27A], Y. Ban[42,g], V. Batozskaya[1,40], D. Becker[31], K. Begzsuren[29], N. Berger[31], M. Bertani[26A], D. Bettoni[27A], F. Bianchi[69A,69C], J. Bloms[63], A. Bortone[69A,69C], I. Boyko[32], R. A. Briere[5], A. Brueggemann[63], H. Cai[71], X. Cai[1,53], A. Calcaterra[26A], G. F. Cao[1,58], N. Cao[1,58], S. A. Cetin[57A], J. F. Chang[1,53], W. L. Chang[1,58], G. Chelkov[32,a], C. Chen[39], Chao Chen[50], G. Chen[1], H. S. Chen[1,58], M. L. Chen[1,53], S. J. Chen[38], S. M. Chen[56], T. Chen[1], X. R. Chen[28,58], X. T. Chen[1], Y. B. Chen[1,53], Z. J. Chen[23,h], W. S. Cheng[69C], S. K. Choi [50], X. Chu[39], G. Cibinetto[27A], F. Cossio[69C], J. J. Cui[45], H. L. Dai[1,53], J. P. Dai[73], A. Dbeyssi[17], R. E. de Boer[4], D. Dedovich[32], Z. Y. Deng[1], A. Denig[31], I. Denysenko[32], M. Destefanis[69A,69C], F. De Mori[69A,69C], Y. Ding[36], J. Dong[1,53], L. Y. Dong[1,58], M. Y. Dong[1,53,58], X. Dong[71], S. X. Du[75], P. Egorov[32,a], Y. L. Fan[71], J. Fang[1,53], S. S. Fang[1,58], W. X. Fang[1], Y. Fang[1], R. Farinelli[27A], L. Fava[69B,69C], F. Feldbauer[4], G. Felici[26A], C. Q. Feng[66,53], J. H. Feng[54], K Fischer[64], M. Fritsch[4], C. Fritzsch[63], C. D. Fu[1], H. Gao[58], Y. N. Gao[42,g], Yang Gao[66,53], S. Garbolino[69C], I. Garzia[27A,27B], P. T. Ge[71], Z. W. Ge[38], C. Geng[54], E. M. Gersabeck[62], A Gilman[64], K. Goetzen[12], L. Gong[36], W. X. Gong[1,53], W. Gradl[31], M. Greco[69A,69C], L. M. Gu[38], M. H. Gu[1,53], Y. T. Gu[14], C. Y Guan[1,58], A. Q. Guo[28,58], L. B. Guo[37], R. P. Guo[44], Y. P. Guo[10,f], A. Guskov[32,a], T. T. Han[45], W. Y. Han[35], X. Q. Hao[18], F. A. Harris[60], K. K. He[50], K. L. He[1,58], F. H. Heinsius[4], C. H. Heinz[31], Y. K. Heng[1,53,58], C. Herold[55], G. Y. Hou[1,58], Y. R. Hou[58], Z. L. Hou[1], H. M. Hu[1,58], J. F. Hu[51,i], T. Hu[1,53,58], Y. Hu[1], G. S. Huang[66,53], K. X. Huang[54], L. Q. Huang[28,58], X. T. Huang[45], Y. P. Huang[1], Z. Huang[42,g], T. Hussain[68], N Hüsken[25,31], W. Imoehl[25], M. Irshad[66,53], J. Jackson[25], S. Jaeger[4], S. Janchiv[29], E. Jang[50], J. H. Jeong[50], Q. Ji[1], Q. P. Ji[18], X. B. Ji[1,58], X. L. Ji[1,53], Y. Y. Ji[45], Z. K. Jia[66,53], H. B. Jiang[45], S. S. Jiang[35], X. S. Jiang[1,53,58], Y. Jiang[58], J. B. Jiao[45], Z. Jiao[21], S. Jin[38], Y. Jin[61], M. Q. Jing[1,58], T. Johansson[70], N. Kalantar-Nayestanaki[59], X. S. Kang[36], R. Kappert[59], M. Kavatsyuk[59], B. C. Ke[75], I. K. Keshk[4], A. Khoukaz[63], R. Kiuchi[1], R. Kliemt[12], L. Koch[33], O. B. Kolcu[57A], B. Kopf[4], M. Kuemmel[4], M. Kuessner[4], A. Kupsc[40,70], W. Kühn[33], J. J. Lane[62], J. S. Lange[33], P. Larin[17], A. Lavania[24], L. Lavezzi[69A,69C], Z. H. Lei[66,53], H. Leithoff[31], M. Lellmann[31], T. Lenz[31], C. Li[39], C. Li[43], C. H. Li[35], Cheng Li[66,53], D. M. Li[75], F. Li[1,53], G. Li[1], H. Li[47], H. Li[66,53], H. B. Li[1,58], H. J. Li[18], H. N. Li[51,i], J. Q. Li[4], J. S. Li[54], J. W. Li[45], Ke Li[1], L. J Li[1], L. K. Li[1], Lei Li[3], M. H. Li[39], P. R. Li[34,j,k], S. X. Li[10], S. Y. Li[56], T. Li[45], W. D. Li[1,58], W. G. Li[1], X. H. Li[66,53], X. L. Li[45], Xiaoyu Li[1,58], Y. G. Li[42,g], Z. X. Li[14], H. Liang[66,53], H. Liang[30], H. Liang[1,58], Y. F. Liang[49], Y. T. Liang[28,58], G. R. Liao[13], L. Z. Liao[45], J. Libby[24], A. Limphirat[55], C. X. Lin[54], D. X. Lin[28,58], T. Lin[1], B. J. Liu[1], C. X. Liu[1], D. Liu[17,66], F. H. Liu[48], Fang Liu[1], Feng Liu[6], G. M. Liu[51,i], H. Liu[34,j,k], H. B. Liu[14], H. M. Liu[1,58], Huanhuan Liu[1], Huihui Liu[19], J. B. Liu[66,53], J. L. Liu[67], J. Y. Liu[1,58], K. Liu[1], K. Y. Liu[36], Ke Liu[20], L. Liu[66,53], Lu Liu[39], M. H. Liu[10,f], P. L. Liu[1], Q. Liu[58], S. B. Liu[66,53], T. Liu[10,f], W. K. Liu[39], W. M. Liu[66,53], X. Liu[34,j,k], Y. Liu[34,j,k], Y. B. Liu[39], Z. A. Liu[1,53,58], Z. Q. Liu[45], X. C. Lou[1,53,58], F. X. Lu[54], H. J. Lu[21], J. G. Lu[1,53], X. L. Lu[1], Y. Lu[7], Y. P. Lu[1,53], Z. H. Lu[1], C. L. Luo[37], M. X. Luo[74], T. Luo[10,f], X. L. Luo[1,53], X. R. Lyu[58], Y. F. Lyu[39], F. C. Ma[36], H. L. Ma[1], L. L. Ma[45], M. M. Ma[1,58], Q. M. Ma[1], R. Q. Ma[1,58], R. T. Ma[58], X. Y. Ma[1,53], Y. Ma[42,g], F. E. Maas[17], M. Maggiora[69A,69C], S. Maldaner[4], S. Malde[64], Q. A. Malik[68], A. Mangoni[26B], Y. J. Mao[42,g], Z. P. Mao[1], S. Marcello[69A,69C], Z. X. Meng[61], J. Messchendorp[12,59], G. Mezzadri[27A], H. Miao[1], T. J. Min[38], R. E. Mitchell[25], X. H. Mo[1,53,58], N. Yu. Muchnoi[11,b], Y. Nefedov[32], F. Nerling[17,d], I. B. Nikolaev[11,b], Z. Ning[1,53], S. Nisar[9,l], Y. Niu [45], S. L. Olsen[58], Q. Ouyang[1,53,58], S. Pacetti[26B,26C], X. Pan[10,f], Y. Pan[52], A. Pathak[30], M. Pelizaeus[4], H. P. Peng[66,53], K. Peters[12,d], J. L. Ping[37], R. G. Ping[1,58], S. Plura[31], S. Pogodin[32], V. Prasad[66,53], F. Z. Qi[1], H. Qi[66,53], H. R. Qi[56], M. Qi[38], T. Y. Qi[10,f], S. Qian[1,53], W. B. Qian[58], Z. Qian[54], C. F. Qiao[58], J. J. Qin[67], L. Q. Qin[13], X. P. Qin[10,f], X. S. Qin[45], Z. H. Qin[1,53], J. F. Qiu[1], S. Q. Qu[39], S. Q. Qu[56], K. H. Rashid[68], C. F. Redmer[31], K. J. Ren[35], A. Rivetti[69C], V. Rodin[59], M. Rolo[69C], G. Rong[1,58], Ch. Rosner[17], S. N. Ruan[39], H. S. Sang[66], A. Sarantsev[32,c], Y. Schelhaas[31], C. Schnier[4], K. Schoenning[70], M. Scodeggio[27A,27B], K. Y. Shan[10,f], W. Shan[22], X. Y. Shan[66,53], J. F. Shangguan[50], L. G. Shao[1,58], M. Shao[66,53], C. P. Shen[10,f], H. F. Shen[1,58], X. Y. Shen[1,58], B. A. Shi[58], H. C. Shi[66,53], J. Y. Shi[1], q. q. Shi[50], R. S. Shi[1,58], X. Shi[1,53], X. D Shi[66,53], J. J. Song[18], W. M. Song[30,1], Y. X. Song[42,g], S. Sosio[69A,69C], S. Spataro[69A,69C], F. Stieler[31], K. X. Su[71], P. P. Su[50], Y. J. Su[58], G. X. Sun[1], H. Sun[58], H. K. Sun[1], J. F. Sun[18], L. Sun[71], S. S. Sun[1,58], T. Sun[1,58], W. Y. Sun[30], X Sun[23,h], Y. J. Sun[66,53], Y. Z. Sun[1], Z. T. Sun[45], Y. H. Tan[71], Y. X. Tan[66,53], C. J. Tang[49], G. Y. Tang[1], J. Tang[54], L. Y Tao[67], Q. T. Tao[23,h], M. Tat[64], J. X. Teng[66,53], V. Thoren[70], W. H. Tian[47], Y. Tian[28,58], I. Uman[57B], B. Wang[1], B. L. Wang[58], C. W. Wang[38], D. Y. Wang[42,g], F. Wang[67], H. J. Wang[34,j,k], H. P. Wang[1,58], K. Wang[1,53], L. L. Wang[1], M. Wang[45], M. Z. Wang[42,g], Meng Wang[1,58], S. Wang[13], S. Wang[10,f], T. Wang[10,f], T. J. Wang[39], W. Wang[54], W. H. Wang[71], W. P. Wang[66,53], X. Wang[42,g], X. F. Wang[34,j,k], X. L. Wang[10,f], Y. Wang[56], Y. D. Wang[41], Y. F. Wang[1,53,58], Y. H. Wang[43], Y. Q. Wang[1], Yaqian Wang[16,1], Z. Wang[1,53], Z. Y. Wang[1,58], Ziyi Wang[58], D. H. Wei[13], F. Weidner[63], S. P. Wen[1], D. J. White[62], U. Wiedner[4], G. Wilkinson[64], M. Wolke[70], L. Wollenberg[4], J. F. Wu[1,58], L. H. Wu[1], L. J. Wu[1,58], X. Wu[10,f],

X. H. Wu[30], Y. Wu[66], Y. J Wu[28], Z. Wu[1,53], L. Xia[66,53], T. Xiang[42,g], D. Xiao[34,j,k], G. Y. Xiao[38], H. Xiao[10,f], S. Y. Xiao[1], Y. L. Xiao[10,f], Z. J. Xiao[37], C. Xie[38], X. H. Xie[42,g], Y. Xie[45], Y. G. Xie[1,53], Y. H. Xie[6], Z. P. Xie[66,53], T. Y. Xing[1,58], C. F. Xu[1], C. J. Xu[54], G. F. Xu[1], H. Y. Xu[61], Q. J. Xu[15], X. P. Xu[50], Y. C. Xu[58], Z. P. Xu[38], F. Yan[10,f], L. Yan[10,f], W. B. Yan[66,53], W. C. Yan[75], H. J. Yang[46,e], H. L. Yang[30], H. X. Yang[1], L. Yang[47], S. L. Yang[58], Tao Yang[1], Y. F. Yang[39], Y. X. Yang[1,58], Yifan Yang[1,58], M. Ye[1,53], M. H. Ye[8], J. H. Yin[1], Z. Y. You[54], B. X. Yu[1,53,58], C. X. Yu[39], G. Yu[1,58], T. Yu[67], X. D. Yu[42,g], C. Z. Yuan[1,58], L. Yuan[2], S. C. Yuan[1], X. Q. Yuan[1], Y. Yuan[1,58], Z. Y. Yuan[54], C. X. Yue[35], A. A. Zafar[68], F. R. Zeng[45], X. Zeng[6], Y. Zeng[23,h], Y. H. Zhan[54], A. Q. Zhang[1], B. L. Zhang[1], B. X. Zhang[1], D. H. Zhang[39], G. Y. Zhang[18], H. Zhang[66], H. H. Zhang[30], H. H. Zhang[54], H. Y. Zhang[1,53], J. L. Zhang[72], J. Q. Zhang[37], J. W. Zhang[1,53,58], J. X. Zhang[34,j,k], J. Y. Zhang[1], J. Z. Zhang[1,58], Jianyu Zhang[1,58], Jiawei Zhang[1,58], L. M. Zhang[56], L. Q. Zhang[54], Lei Zhang[38], P. Zhang[1], Q. Y. Zhang[35,75], Shuihan Zhang[1,58], Shulei Zhang[23,h], X. D. Zhang[41], X. M. Zhang[1], X. Y. Zhang[45], X. Y. Zhang[50], Y. Zhang[64], Y. T. Zhang[75], Y. H. Zhang[1,53], Yan Zhang[66,53], Yao Zhang[1], Z. H. Zhang[1], Z. Y. Zhang[39], Z. Y. Zhang[71], G. Zhao[1], J. Zhao[35], J. Y. Zhao[1,58], J. Z. Zhao[1,53], Lei Zhao[66,53], Ling Zhao[1], M. G. Zhao[39], S. J. Zhao[75], Y. B. Zhao[1,53], Y. X. Zhao[28,58], Z. G. Zhao[66,53], A. Zhemchugov[32,a], B. Zheng[67], J. P. Zheng[1,53], Y. H. Zheng[58], B. Zhong[37], C. Zhong[67], X. Zhong[54], H. Zhou[45], L. P. Zhou[1,58], X. Zhou[71], X. K. Zhou[58], X. R. Zhou[66,53], X. Y. Zhou[35], Y. Z. Zhou[10,f], J. Zhu[39], K. Zhu[1], K. J. Zhu[1,53,58], L. X. Zhu[58], S. H. Zhu[65], S. Q. Zhu[38], T. J. Zhu[72], W. J. Zhu[10,f], Y. C. Zhu[66,53], Z. A. Zhu[1,58], J. H. Zou[1]

(BESIII Collaboration)

[1] *Institute of High Energy Physics, Beijing 100049, People's Republic of China*
[2] *Beihang University, Beijing 100191, People's Republic of China*
[3] *Beijing Institute of Petrochemical Technology, Beijing 102617, People's Republic of China*
[4] *Bochum Ruhr-University, D-44780 Bochum, Germany*
[5] *Carnegie Mellon University, Pittsburgh, Pennsylvania 15213, USA*
[6] *Central China Normal University, Wuhan 430079, People's Republic of China*
[7] *Central South University, Changsha 410083, People's Republic of China*
[8] *China Center of Advanced Science and Technology, Beijing 100190, People's Republic of China*
[9] *COMSATS University Islamabad, Lahore Campus, Defence Road, Off Raiwind Road, 54000 Lahore, Pakistan*
[10] *Fudan University, Shanghai 200433, People's Republic of China*
[11] *G.I. Budker Institute of Nuclear Physics SB RAS (BINP), Novosibirsk 630090, Russia*
[12] *GSI Helmholtzcentre for Heavy Ion Research GmbH, D-64291 Darmstadt, Germany*
[13] *Guangxi Normal University, Guilin 541004, People's Republic of China*
[14] *Guangxi University, Nanning 530004, People's Republic of China*
[15] *Hangzhou Normal University, Hangzhou 310036, People's Republic of China*
[16] *Hebei University, Baoding 071002, People's Republic of China*
[17] *Helmholtz Institute Mainz, Staudinger Weg 18, D-55099 Mainz, Germany*
[18] *Henan Normal University, Xinxiang 453007, People's Republic of China*
[19] *Henan University of Science and Technology, Luoyang 471003, People's Republic of China*
[20] *Henan University of Technology, Zhengzhou 450001, People's Republic of China*
[21] *Huangshan College, Huangshan 245000, People's Republic of China*
[22] *Hunan Normal University, Changsha 410081, People's Republic of China*
[23] *Hunan University, Changsha 410082, People's Republic of China*
[24] *Indian Institute of Technology Madras, Chennai 600036, India*
[25] *Indiana University, Bloomington, Indiana 47405, USA*
[26] *INFN Laboratori Nazionali di Frascati , (A)INFN Laboratori Nazionali di Frascati, I-00044, Frascati, Italy; (B)INFN Sezione di Perugia, I-06100, Perugia, Italy; (C)University of Perugia, I-06100, Perugia, Italy*
[27] *INFN Sezione di Ferrara, (A)INFN Sezione di Ferrara, I-44122, Ferrara, Italy; (B)University of Ferrara, I-44122, Ferrara, Italy*
[28] *Institute of Modern Physics, Lanzhou 730000, People's Republic of China*
[29] *Institute of Physics and Technology, Peace Avenue 54B, Ulaanbaatar 13330, Mongolia*
[30] *Jilin University, Changchun 130012, People's Republic of China*
[31] *Johannes Gutenberg University of Mainz, Johann-Joachim-Becher-Weg 45, D-55099 Mainz, Germany*
[32] *Joint Institute for Nuclear Research, 141980 Dubna, Moscow region, Russia*
[33] *Justus-Liebig-Universitaet Giessen, II. Physikalisches Institut, Heinrich-Buff-Ring 16, D-35392 Giessen, Germany*
[34] *Lanzhou University, Lanzhou 730000, People's Republic of China*

[35] Liaoning Normal University, Dalian 116029, People's Republic of China
[36] Liaoning University, Shenyang 110036, People's Republic of China
[37] Nanjing Normal University, Nanjing 210023, People's Republic of China
[38] Nanjing University, Nanjing 210093, People's Republic of China
[39] Nankai University, Tianjin 300071, People's Republic of China
[40] National Centre for Nuclear Research, Warsaw 02-093, Poland
[41] North China Electric Power University, Beijing 102206, People's Republic of China
[42] Peking University, Beijing 100871, People's Republic of China
[43] Qufu Normal University, Qufu 273165, People's Republic of China
[44] Shandong Normal University, Jinan 250014, People's Republic of China
[45] Shandong University, Jinan 250100, People's Republic of China
[46] Shanghai Jiao Tong University, Shanghai 200240, People's Republic of China
[47] Shanxi Normal University, Linfen 041004, People's Republic of China
[48] Shanxi University, Taiyuan 030006, People's Republic of China
[49] Sichuan University, Chengdu 610064, People's Republic of China
[50] Soochow University, Suzhou 215006, People's Republic of China
[51] South China Normal University, Guangzhou 510006, People's Republic of China
[52] Southeast University, Nanjing 211100, People's Republic of China
[53] State Key Laboratory of Particle Detection and Electronics, Beijing 100049, Hefei 230026, People's Republic of China
[54] Sun Yat-Sen University, Guangzhou 510275, People's Republic of China
[55] Suranaree University of Technology, University Avenue 111, Nakhon Ratchasima 30000, Thailand
[56] Tsinghua University, Beijing 100084, People's Republic of China
[57] Turkish Accelerator Center Particle Factory Group, (A)Istinye University, 34010, Istanbul, Turkey; (B)Near East University, Nicosia, North Cyprus, Mersin 10, Turkey
[58] University of Chinese Academy of Sciences, Beijing 100049, People's Republic of China
[59] University of Groningen, NL-9747 AA Groningen, The Netherlands
[60] University of Hawaii, Honolulu, Hawaii 96822, USA
[61] University of Jinan, Jinan 250022, People's Republic of China
[62] University of Manchester, Oxford Road, Manchester, M13 9PL, United Kingdom
[63] University of Muenster, Wilhelm-Klemm-Strasse 9, 48149 Muenster, Germany
[64] University of Oxford, Keble Road, Oxford OX13RH, United Kingdom
[65] University of Science and Technology Liaoning, Anshan 114051, People's Republic of China
[66] University of Science and Technology of China, Hefei 230026, People's Republic of China
[67] University of South China, Hengyang 421001, People's Republic of China
[68] University of the Punjab, Lahore-54590, Pakistan
[69] University of Turin and INFN, (A)University of Turin, I-10125, Turin, Italy; (B)University of Eastern Piedmont, I-15121, Alessandria, Italy; (C)INFN, I-10125, Turin, Italy
[70] Uppsala University, Box 516, SE-75120 Uppsala, Sweden
[71] Wuhan University, Wuhan 430072, People's Republic of China
[72] Xinyang Normal University, Xinyang 464000, People's Republic of China
[73] Yunnan University, Kunming 650500, People's Republic of China
[74] Zhejiang University, Hangzhou 310027, People's Republic of China
[75] Zhengzhou University, Zhengzhou 450001, People's Republic of China

[a] Also at the Moscow Institute of Physics and Technology, Moscow 141700, Russia
[b] Also at the Novosibirsk State University, Novosibirsk, 630090, Russia
[c] Also at the NRC "Kurchatov Institute", PNPI, 188300, Gatchina, Russia
[d] Also at Goethe University Frankfurt, 60323 Frankfurt am Main, Germany
[e] Also at Key Laboratory for Particle Physics, Astrophysics and Cosmology, Ministry of Education; Shanghai Key Laboratory for Particle Physics and Cosmology; Institute of Nuclear and Particle Physics, Shanghai 200240, People's Republic of China
[f] Also at Key Laboratory of Nuclear Physics and Ion-beam Application (MOE) and Institute of Modern Physics, Fudan University, Shanghai 200443, People's Republic of China
[g] Also at State Key Laboratory of Nuclear Physics and Technology, Peking University, Beijing 100871, People's Republic of China

[h] Also at School of Physics and Electronics, Hunan University, Changsha 410082, China
[i] Also at Guangdong Provincial Key Laboratory of Nuclear Science, Institute of Quantum Matter, South China Normal University, Guangzhou 510006, China
[j] Also at Frontiers Science Center for Rare Isotopes, Lanzhou University, Lanzhou 730000, People's Republic of China
[k] Also at Lanzhou Center for Theoretical Physics, Lanzhou University, Lanzhou 730000, People's Republic of China
[l] Also at the Department of Mathematical Sciences, IBA, Karachi , Pakistan

Cross sections for the process $e^+e^- \to K_S^0 K_S^0 J/\psi$ at center-of-mass energies from 4.128 to 4.950 GeV are measured using data samples with a total integrated luminosity of 21.2 fb^{-1} collected by the BESIII detector operating at the BEPCII storage ring. The $Y(4230)$ state is observed in the energy dependence of the $e^+e^- \to K_S^0 K_S^0 J/\psi$ cross section for the first time with a statistical significance of 26.0σ. In addition, an enhancement around 4.710 GeV, called the $Y(4710)$, is seen with a statistical significance of 4.2σ. There is no clear structure around 4.484 GeV. Using a fit with a coherent sum of three Breit-Wigner functions, we determine the mass and width of the $Y(4230)$ state to be $4226.9 \pm 6.6 \pm 22.0$ MeV/c^2 and $71.7 \pm 16.2 \pm 32.8$ MeV, respectively, and the mass and width of the $Y(4710)$ state to be $4704.0 \pm 52.3 \pm 69.5$ MeV/c^2 and $183.2 \pm 114.0 \pm 96.1$ MeV, respectively, where the first uncertainties are statistical and the second are systematic. In addition, the average Born cross section ratio of $e^+e^- \to K_S^0 K_S^0 J/\psi$ to $e^+e^- \to K^+K^- J/\psi$ is measured to be $0.388^{+0.035}_{-0.028} \pm 0.016$, or $0.426^{+0.038}_{-0.031} \pm 0.018$ if three-body phase space is considered.

PACS numbers: 14.20.Pt, 14.40.Lb, 13.25.Gv, 13.25.Es

I. INTRODUCTION

In the past two decades, a series of charmonium-like states have been discovered that do not fit into the spectrum predicted by the conventional quark model [1]. The existence of these states challenges our understanding of both charmonium spectroscopy and QCD calculations [2, 3]. In particular, the number of observed vector states with masses above open-charm threshold is more than that expected for conventional charmonium states, and this implies the existence of exotic states beyond the quark-antiquark meson picture. In addition to the three well-established charmonium states above the $\psi(3770)$, the $\psi(4040)$, $\psi(4160)$, and $\psi(4415)$ [4], other experimentally discovered Y states, such as the $Y(4230)$, overpopulate the conventional charmonium spectrum. These Y states have not yet been found to decay to $D\bar{D}$, although their masses are above $D\bar{D}$ threshold [5, 6]. The $Y(4230)$ state was discovered via the process $e^+e^- \to \pi^+\pi^- J/\psi$ by the BaBar experiment [7] using initial state radiation (ISR) and then confirmed by the CLEO [8] and Belle experiments [9]. Several theoretical interpretations have been proposed for the $Y(4230)$ state, such as tetraquark [10], meson molecule [11, 12], hadroquarkonium [13, 14], hybrid meson [15–17], and others [18–21].

The BESIII experiment has previously studied Y states via e^+e^- cross section measurements using various hidden-charm decay modes, such as $e^+e^- \to \pi\pi J/\psi$ [22, 23], $\pi^+\pi^- h_c$ [24], $\pi\pi\psi(2S)$ [25–27], $\omega\chi_{c0}$ [28, 29], $K^+K^- J/\psi$ [30, 31], and so on. Recently, in a study of the cross sections of the process $e^+e^- \to K^+K^- J/\psi$ at center-of-mass (CM) energies ($\sqrt{s}$) below 4.600 GeV, the BESIII experiment reported two structures, the $Y(4230)$ and $Y(4500)$ [31]. The $K^+K^- J/\psi$ decay mode of the $Y(4230)$ state was first seen by the CLEO experiment [8] in 2006. Later, the Belle experiment measured the Born cross section of $K^+K^- J/\psi$ via ISR [32, 33], but failed to confirm the decay $Y(4230) \to K^+K^- J/\psi$ due to limited data sample size. The $Y(4500)$ is a new structure that was first observed at BESIII with a statistical significance of 8σ and its mass and width were measured to be $4484.7 \pm 13.3 \pm 24.1$ MeV/c^2 and $111.1 \pm 30.1 \pm 15.2$ MeV, respectively [31]. The neutral process $e^+e^- \to K_S^0 K_S^0 J/\psi$ is a good probe to investigate the $Y(4500)$ state. The Belle experiment measured the cross sections of $e^+e^- \to K_S^0 K_S^0 J/\psi$ [32, 33], but only upper limits were given. Also, using data samples from $\sqrt{s} = 4.189$ to 4.600 MeV, corresponding to an integrated luminosity of 4.7 fb^{-1}, the BESIII experiment performed a measurement of the Born cross sections of $e^+e^- \to K_S^0 K_S^0 J/\psi$ at fourteen energy points [30], and measured non-zero Born cross sections at seven of those energy points [30]. No structure was observed in the measured Born cross sections of $e^+e^- \to K_S^0 K_S^0 J/\psi$. In addition, Ref. [30] reported the Born cross section ratio of $e^+e^- \to K_S^0 K_S^0 J/\psi$ to $e^+e^- \to K^+K^- J/\psi$ to be $\frac{\sigma^{\rm Born}(K_S^0 K_S^0 J/\psi)}{\sigma^{\rm Born}(K^+K^- J/\psi)} = 0.370^{+0.064}_{-0.058} \pm 0.042$, where the first uncertainty is statistical and the second is systematic.

In this paper, we present a follow-up study of $e^+e^- \to K_S^0 K_S^0 J/\psi$ at $\sqrt{s}$ from 4.128 to 4.950 GeV using data samples corresponding to a total integrated luminosity ($\mathcal{L}$) of 21.2 fb^{-1} [34–37] collected at thirty-six energy points by the BESIII detector [38].

II. THE BESIII DETECTOR AND DATA SAMPLES

The BESIII detector [38] records symmetric e^+e^- collisions provided by the BEPCII storage ring [39] in the CM energy range from 2.0 to 4.95 GeV, with a peak luminosity of 1×10^{33} cm^{-2}s^{-1} achieved at $\sqrt{s} = 3.77$ GeV. BESIII has collected large data samples in this energy region [40]. The cylindrical core of the BESIII detector covers 93% of the full solid angle and consists of a helium-based multilayer drift chamber (MDC), a plastic scintillator time-of-flight system (TOF), and a CsI(Tl) electromagnetic calorimeter (EMC), which are all enclosed in a superconducting solenoidal magnet providing a 1.0 T magnetic field [41]. The solenoid is supported by an octagonal flux-return yoke with resistive plate counter muon identification modules interleaved with steel. The charged-particle momentum resolution at 1 GeV/c is 0.5%, and the $\mathrm{d}E/\mathrm{d}x$ resolution is 6% for electrons from Bhabha scattering. The EMC measures photon energies with a resolution of 2.5% (5%) at 1 GeV in the barrel (end cap) region. The time resolution in the TOF barrel region is 68 ps, while that in the end cap region is 110 ps. The end cap TOF system was upgraded in 2015 using multigap resistive plate chamber technology, providing a time resolution of 60 ps [42].

Simulated data samples produced with a GEANT4-based [43] Monte Carlo (MC) toolkit, which includes the geometric description of the BESIII detector and the detector response, are used to determine detection efficiencies and to estimate backgrounds. The simulation models the beam energy spread and ISR in the e^+e^- annihilations with the generator KKMC [44, 45]. The inclusive MC sample includes the production of open charm processes, the ISR production of vector charmonium(-like) states, and the continuum processes incorporated in KKMC [44, 45]. All particle decays are modelled with EVTGEN [46, 47] using branching fractions either taken from the Particle Data Group (PDG) [4], when available, or otherwise estimated with LUNDCHARM [48, 49]. Final state radiation from charged final state particles is incorporated using PHOTOS [50]. Signal MC samples are generated for $e^+e^- \to K_S^0 K_S^0 J/\psi$ using EVTGEN [46, 47] and assuming a uniform distribution in the available phase space. KKMC [44, 45] is used to calculate the ISR correction factors needed to convert an observed cross section to a Born cross section [51, 52].

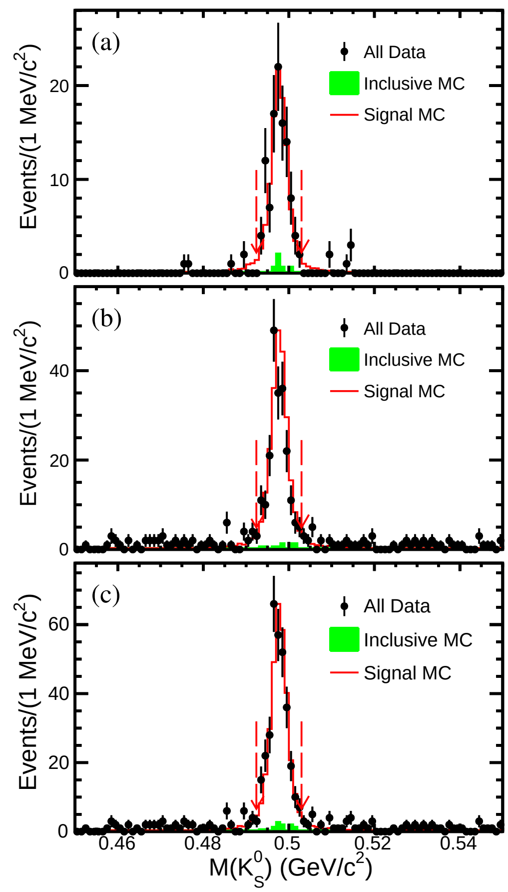

FIG. 1. The reconstructed K_S^0 mass $M(K_S^0)$ for (a) the two-K_S^0 reconstruction method, (b) the one-K_S^0 reconstruction method, and (c) both methods. Data from all CM energies are combined. The dots with error bars are data, the green filled histograms are the background from inclusive MC samples, and the red histograms are signal MC samples. The average signal regions are shown by the red arrows.

III. DATA ANALYSIS

We reconstruct the final state $K_S^0 K_S^0 J/\psi$, where the J/ψ decays into a lepton pair (e^+e^- or $\mu^+\mu^-$), and one K_S^0 decays into $\pi^+\pi^-$ while the other K_S^0 decays into either $\pi^+\pi^-$ or $\pi^0\pi^0$. For events with six charged tracks, full reconstruction is performed (the "two-K_S^0" reconstruction method). For events with four or five charged tracks, partial reconstruction is performed (the "one-K_S^0" reconstruction method).

A charged lepton candidate (e or μ) must have a distance of closest approach to the interaction point (IP) less than 10 cm along the z-axis ($|V_z| < 10.0$ cm) and less than 1 cm in the transverse plane ($|V_{xy}| < 1$ cm), and a polar angle (θ) range of $|\cos\theta| < 0.93$. The z-axis is the symmetry axis of the MDC, and θ is defined with respect to the z-axis. In addition, the absolute momentum of a lepton candidate is required to be greater than 0.95 GeV/c ($P > 0.95$ GeV/c). A lepton with energy deposited in the calorimeter greater than 0.95 GeV is assigned as an electron, otherwise a muon.

A K_S^0 candidate is reconstructed from two oppositely charged tracks satisfying $|V_z| < 20$ cm and $P < 0.95$ GeV/c. The two charged tracks are assigned as $\pi^+\pi^-$ without imposing further particle identification criteria. They are constrained to originate from a common vertex, and the decay length of the K_S^0 candidate is required to be greater than twice the vertex resolution away from the IP. The K_S^0 candidate is required to have an invariant mass of $\pi^+\pi^-$ within $(m_{K_S^0} - 3\sigma_{K_S^0}, m_{K_S^0} + 3\sigma_{K_S^0})$, where $m_{K_S^0}$ and $\sigma_{K_S^0}$ are the fitted mean and width of a signal Gaussian function fit to the signal MC samples. The value of $m_{K_S^0}$ increases from 497.6 to 498.0 MeV/c^2 for different CM energies, while $\sigma_{K_S^0}$ varies from 1.3 to 2.4 MeV/c^2. The reconstructed K_S^0 mass spectra $M(K_S^0)$ are shown in Fig. 1.

A photon candidate, originating from π^0 decay, is identified using showers in the EMC. The deposited energy of the shower must be more than 25 MeV in the barrel region ($|\cos\theta| < 0.8$), and more than 50 MeV in the end cap region ($0.86 < |\cos\theta| < 0.92$). To exclude a shower that originates from a charged track, the angle subtended by the EMC shower and the position of the closest charged track at the EMC must be greater than 10 degrees as measured from the IP. To suppress electronic noise and showers unrelated to the event, the difference between the EMC time and the event start time is required to be within [0, 700] ns. For the case with four charged tracks (two charged pions and two leptons), the number of photons (N_γ) is required to be not less than two.

To suppress potential background and improve resolution, a four-constraint (4C) kinematic fit is performed in the case of the two-K_S^0 reconstruction method, while a one-constraint (1C) kinematic fit is used in the one-K_S^0 reconstruction method. For the 4C fit, the the total final-state four-momentum is constrained to the initial CM system. For the 1C fit, the missing mass is constrained to the known K_S^0 mass. The χ^2 of the kinematic fit is required to be less than 200 for the 4C fit and less than 20 for the 1C fit. Both requirements on the χ^2 of the kinematic fit have been optimized using the figure-of-merit (FOM) $\frac{S}{\sqrt{S+B}}$, where S is the signal yield that is estimated by the signal MC samples and normalized by the previously measured cross sections, and B is the background yield that is estimated by the inclusive MC samples and normalized according to the luminosities. The optimization is performed in the signal region, which is defined as $M(l^+l^-) \in (m_{J/\psi} - 3\sigma_{J/\psi}, m_{J/\psi} + 3\sigma_{J/\psi})$ for both the one-K_S^0 and two-K_S^0 reconstruction methods, where $M(l^+l^-)$ is the invariant mass of the lepton pair, and $m_{J/\psi}$ and $\sigma_{J/\psi}$ are the mean and width of a signal Gaussian function fit to the signal MC samples. The value of $m_{J/\psi}$ is around 3097.3 MeV/c^2, while $\sigma_{J/\psi}$ increases from 3.4 to 6.8 MeV/c^2 for different CM energies. In addition, the sideband regions of $M(l^+l^-)$ are defined as $(m_{J/\psi} - 13\sigma_{J/\psi}, m_{J/\psi} - 7\sigma_{J/\psi})$ and $(m_{J/\psi} + 7\sigma_{J/\psi}, m_{J/\psi} + 13\sigma_{J/\psi})$. Therefore, the normalized ratio of sideband to signal regions is 0.50.

After imposing the above requirements, the $M(l^+l^-)$ distributions for all CM energies combined are shown in Fig. 2. Obvious J/ψ signal peaks can be seen. Figure 2(a) and 2(b) are for the two-K_S^0 and one-K_S^0 reconstruction methods, respectively. The numbers of signal events for all CM energies are estimated to be 107.4 ± 10.4 for the two-K_S^0 reconstruction method and 237.6 ± 16.9 for the one-K_S^0 reconstruction method, where the uncertainties are statistical only. The total number of signal events is then taken as the sum of those from the two reconstruction methods. According to studies based on all inclusive MC samples, there is no significant peaking background.

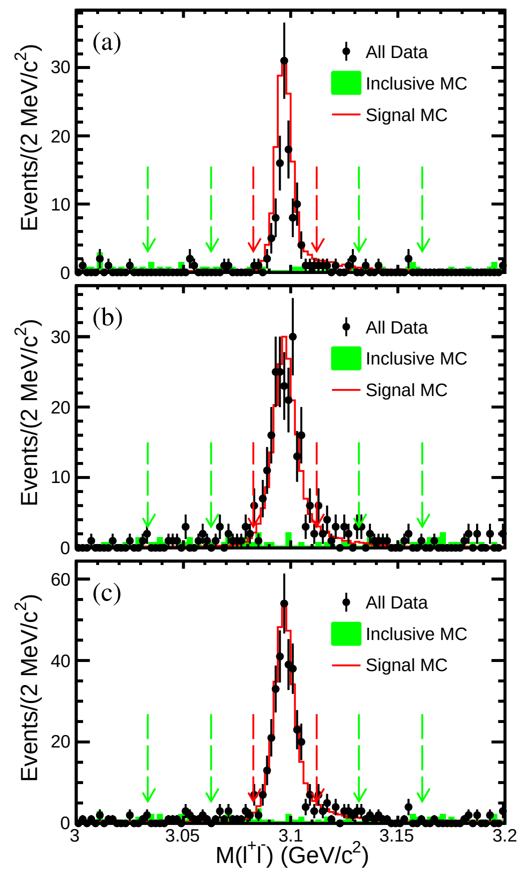

FIG. 2. The invariant mass of the lepton pair $M(l^+l^-)$ for (a) the two-K_S^0 reconstruction method, (b) the one-K_S^0 reconstruction method, and (c) both methods. Data from all CM energies are combined. The dots with error bars are data, the green filled histograms are the background from inclusive MC samples, and the red histograms are signal MC samples. The average signal regions are shown by the red arrows, and the average sideband regions are shown by the green arrows.

IV. CROSS SECTION

The Born cross section $\sigma^{\rm Born}$ at each CM energy is calculated using:

$$\sigma^{\rm Born} \equiv \frac{N_{\rm sig}}{\mathcal{L}\epsilon\mathcal{B}_{J/\psi\to l^+l^-}(1+\delta)\delta^{\rm VP}}, \quad (1)$$

where $N_{\rm sig}$ is the signal yield, calculated by subtracting the number of J/ψ sideband events from the number of J/ψ signal events; ϵ is the event selection efficiency obtained from phase-space modeled signal MC simulations, which includes the K_S^0 decay branching fractions; $\mathcal{B}_{J/\psi\to l^+l^-}$ is the PDG value of the branching fraction of the J/ψ decaying into a lepton pair [4]; $(1+\delta)$ is the ISR correction factor; and $\delta^{\rm VP}$ is the vacuum polarization factor taken from Ref. [53]. Statistical uncertainties on the numbers of signal events are calculated using the Rolke method [54]. In the Rolke method [54], the background is assumed to obey a Poisson distribution. The values for ϵ and $(1+\delta)$ are estimated based on signal MC samples using an iterative weighting method [52]. In the iterations, we describe the dressed cross sections $\sigma^{\rm dress} = \sigma^{\rm Born}\delta^{\rm VP}$ by a coherent sum of three Breit-Wigner functions, as described in the next paragraph. For energy points with statistical significance less than 3σ, upper limits are calculated at a 90% confidence level (C.L.) and include systematic uncertainties determined using the Rolke method [54] with an additional uncertainty on the efficiency. The measured

TABLE I. The CM energies ($\sqrt{s}$), integrated luminosities ($\mathcal{L}$), signal yields ($N_{\rm sig}$), upper limits of signal yields at the 90% C.L. ($N_{\rm ul}$), background yields ($N_{\rm bkg}$), event selection efficiencies (ϵ), ISR correction factors ($(1+\delta)$), vacuum polarization factors ($\delta^{\rm VP}$), Born cross sections ($\sigma^{\rm Born}$), upper limits of cross section at the 90% C.L. for the energy pionts with statistical significance less than 3σ ($\sigma^{\rm ul}$), and the Born cross section ratios ($\frac{\sigma^{\rm Born}(K_S^0K_S^0J/\psi)}{\sigma^{\rm Born}(K^+K^-J/\psi)}$). The first uncertainties of $\sigma^{\rm Born}$ are statistical, and the second ones systematic. The uncertainties of $N_{\rm sig}$ are only statistical.

$\sqrt{s}$ (GeV)	$\mathcal{L}$ (pb^{-1})	$N_{\rm sig}$	$N_{\rm ul}$	$N_{\rm bkg}$	ϵ (%)	$(1+\delta)$	$\delta^{\rm VP}$	$\sigma^{\rm Born}$ (pb)	$\sigma^{\rm ul}$ (pb)	$\frac{\sigma^{\rm Born}(K_S^0K_S^0J/\psi)}{\sigma^{\rm Born}(K^+K^-J/\psi)}$
4.128	401.5	$0.0^{+1.0}_{-0.7}$	2.4	0.0	16.3	0.691	1.052	$0.00^{+0.18}_{-0.12}\pm0.01$	0.5	–
4.157	408.7	$2.0^{+1.8}_{-1.1}$	5.9	0.0	18.4	0.706	1.053	$0.30^{+0.27}_{-0.16}\pm0.03$	1.0	$0.532^{+0.538}_{-0.352}\pm0.022$
4.178	3194.5	$15.0^{+4.4}_{-3.8}$	–	1.0	19.8	0.711	1.054	$0.26^{+0.08}_{-0.07}\pm0.03$	–	$0.380^{+0.123}_{-0.108}\pm0.016$
4.189	526.7	$4.0^{+2.3}_{-1.7}$	–	0.0	20.2	0.712	1.056	$0.42^{+0.24}_{-0.18}\pm0.04$	–	$0.431^{+0.271}_{-0.207}\pm0.018$
4.199	526.0	$1.5^{+2.2}_{-1.5}$	6.1	1.5	20.6	0.713	1.056	$0.15^{+0.23}_{-0.15}\pm0.01$	0.7	$0.115^{+0.170}_{-0.116}\pm0.005$
4.209	517.1	$7.0^{+3.0}_{-2.3}$	–	0.0	20.4	0.716	1.057	$0.74^{+0.32}_{-0.24}\pm0.07$	–	$0.431^{+0.202}_{-0.160}\pm0.018$
4.219	514.6	$19.0^{+4.7}_{-4.0}$	–	0.0	20.9	0.721	1.056	$1.94^{+0.48}_{-0.41}\pm0.18$	–	$0.535^{+0.148}_{-0.129}\pm0.022$
4.226	1100.9	$39.0^{+6.7}_{-6.0}$	–	1.0	21.5	0.733	1.056	$1.79^{+0.31}_{-0.28}\pm0.17$	–	$0.414^{+0.078}_{-0.070}\pm0.017$
4.236	530.3	$10.0^{+3.7}_{-3.1}$	–	1.0	21.3	0.751	1.056	$0.94^{+0.35}_{-0.29}\pm0.09$	–	$0.296^{+0.117}_{-0.099}\pm0.012$
4.244	538.1	$19.0^{+4.9}_{-4.2}$	–	1.0	20.9	0.774	1.056	$1.73^{+0.45}_{-0.38}\pm0.16$	–	$0.505^{+0.145}_{-0.126}\pm0.021$
4.258	828.4	$26.0^{+5.6}_{-4.9}$	–	1.0	20.4	0.821	1.054	$1.49^{+0.32}_{-0.28}\pm0.14$	–	$0.496^{+0.118}_{-0.105}\pm0.021$
4.267	531.1	$14.0^{+4.1}_{-3.4}$	–	0.0	19.9	0.851	1.053	$1.24^{+0.36}_{-0.30}\pm0.12$	–	$0.654^{+0.220}_{-0.186}\pm0.027$
4.278	175.7	$3.0^{+2.1}_{-1.4}$	–	0.0	19.0	0.885	1.053	$0.81^{+0.56}_{-0.38}\pm0.08$	–	$0.376^{+0.284}_{-0.198}\pm0.016$
4.288	502.4	$7.0^{+3.0}_{-2.3}$	–	0.0	18.0	0.914	1.053	$0.67^{+0.29}_{-0.22}\pm0.06$	–	$0.413^{+0.195}_{-0.155}\pm0.017$
4.312	501.0	$5.0^{+3.4}_{-2.9}$	12.0	3.0	17.2	0.968	1.052	$0.48^{+0.32}_{-0.28}\pm0.05$	1.2	$0.442^{+0.321}_{-0.276}\pm0.018$
4.337	505.0	$4.5^{+2.6}_{-2.0}$	–	0.5	17.1	1.002	1.051	$0.41^{+0.24}_{-0.18}\pm0.04$	–	$0.496^{+0.330}_{-0.267}\pm0.021$
4.358	543.9	$5.5^{+3.1}_{-2.5}$	–	1.5	18.0	1.011	1.051	$0.44^{+0.25}_{-0.20}\pm0.04$	–	$0.403^{+0.246}_{-0.203}\pm0.017$
4.377	522.7	$5.0^{+2.9}_{-2.3}$	–	1.0	17.4	0.997	1.051	$0.44^{+0.26}_{-0.20}\pm0.04$	–	$0.296^{+0.184}_{-0.150}\pm0.012$
4.396	507.8	$10.5^{+3.7}_{-3.0}$	–	0.5	18.3	0.966	1.051	$0.93^{+0.33}_{-0.27}\pm0.09$	–	$1.278^{+0.693}_{-0.609}\pm0.053$
4.416	1090.7	$8.0^{+3.8}_{-3.3}$	–	3.0	19.9	0.915	1.052	$0.32^{+0.15}_{-0.13}\pm0.03$	–	$0.262^{+0.132}_{-0.115}\pm0.011$
4.436	569.9	$12.5^{+4.2}_{-3.5}$	–	1.5	20.7	0.862	1.054	$0.98^{+0.33}_{-0.27}\pm0.09$	–	$0.429^{+0.160}_{-0.136}\pm0.018$
4.467	111.1	$1.0^{+1.4}_{-0.7}$	4.0	0.0	22.6	0.816	1.055	$0.39^{+0.54}_{-0.27}\pm0.04$	1.7	$0.129^{+0.185}_{-0.097}\pm0.005$
4.527	112.1	$3.0^{+2.1}_{-1.4}$	–	0.0	21.7	0.913	1.054	$1.08^{+0.75}_{-0.50}\pm0.10$	–	$0.223^{+0.164}_{-0.114}\pm0.009$
4.600	586.9	$10.5^{+3.7}_{-3.0}$	–	0.5	19.4	1.031	1.055	$0.71^{+0.25}_{-0.20}\pm0.07$	–	$0.364^{+0.142}_{-0.119}\pm0.015$
4.612	103.8	$1.0^{+1.4}_{-0.7}$	4.0	0.0	19.0	1.013	1.055	$0.40^{+0.56}_{-0.28}\pm0.04$	1.7	–
4.628	521.5	$1.5^{+2.8}_{-2.0}$	7.2	3.5	19.4	0.977	1.054	$0.12^{+0.22}_{-0.16}\pm0.01$	0.6	–
4.641	552.4	$10.0^{+4.3}_{-3.8}$	–	4.0	20.1	0.944	1.054	$0.76^{+0.33}_{-0.29}\pm0.07$	–	–
4.661	529.6	$9.5^{+4.1}_{-3.6}$	–	3.5	21.3	0.897	1.054	$0.75^{+0.32}_{-0.28}\pm0.07$	–	–
4.682	1669.3	$37.5^{+7.3}_{-6.7}$	–	7.5	22.0	0.864	1.054	$0.94^{+0.18}_{-0.17}\pm0.09$	–	–
4.698	536.5	$14.5^{+4.2}_{-3.6}$	–	0.5	22.7	0.858	1.055	$1.10^{+0.32}_{-0.27}\pm0.10$	–	–
4.740	164.3	$1.5^{+1.8}_{-1.3}$	5.4	0.5	23.6	0.880	1.055	$0.35^{+0.42}_{-0.30}\pm0.03$	1.4	–
4.750	367.2	$12.5^{+4.3}_{-3.8}$	–	2.5	23.5	0.892	1.055	$1.29^{+0.44}_{-0.39}\pm0.12$	–	–
4.780	512.8	$14.0^{+5.1}_{-4.5}$	–	6.0	22.6	0.927	1.055	$1.03^{+0.38}_{-0.33}\pm0.10$	–	–
4.842	527.3	$10.0^{+3.9}_{-3.3}$	–	2.0	21.5	1.000	1.056	$0.70^{+0.27}_{-0.23}\pm0.07$	–	–
4.918	208.1	$3.5^{+2.4}_{-1.8}$	8.6	0.5	20.3	1.063	1.056	$0.62^{+0.42}_{-0.32}\pm0.06$	1.7	–
4.950	160.4	$1.0^{+1.9}_{-1.1}$	4.9	1.0	19.8	1.083	1.056	$0.23^{+0.44}_{-0.25}\pm0.02$	1.2	–

Born cross sections are shown in Fig. 3(a), and the detailed quantities are shown in Table I. The Born cross section ratios $\frac{\sigma^{\rm Born}(K_S^0K_S^0J/\psi)}{\sigma^{\rm Born}(K^+K^-J/\psi)}$ are shown in Fig. 3(b).

A maximum likelihood method is used to fit the dressed cross sections and determine the parameters of the resonant structures. Assuming $K_S^0K_S^0J/\psi$ is produced from three resonances, the cross section is parameterized as a coherent sum of three relativistic Breit-Wigner functions

$$\sigma^{\rm dress}\equiv|BW_1+BW_2e^{i\phi_2}+BW_3e^{i\phi_3}|^2, \qquad (2)$$

where $BW_j\equiv\frac{M_j}{\sqrt{s}}\frac{\sqrt{12\pi(\Gamma_{ee}\mathcal{B})_j\Gamma_j}}{s-M_j^2+iM_j\Gamma_j}\sqrt{\frac{\Phi(\sqrt{s})}{\Phi(M_j)}}$ is the relativistic Breit-Wigner function with j = 1, 2, or 3, and $\Phi(\sqrt{s})$ is the three-body phase-space factor. The mass M_2 and total width Γ_2 are fixed to those of the $Y(4500)$ [31], while the other parameters, *i.e.*, the masses M_j, the total widths Γ_j, the prod-

TABLE II. The fitted parameters of the measured cross sections of $e^+e^- \to K_S^0K_S^0J/\psi$, where the first uncertainties are statistical and the second are systematic. The M_1, Γ_1, and $(\Gamma_{ee}\mathcal{B})_1$ parameters are the mass, width, and $\Gamma_{ee}\mathcal{B}$ for the $Y(4230)$ state; the M_2, Γ_2, $(\Gamma_{ee}\mathcal{B})_2$, and ϕ_2 parameters are for the $Y(4500)$ state; and the M_3, Γ_3, $(\Gamma_{ee}\mathcal{B})_3$, and ϕ_3 parameters are for the $Y(4710)$ state. The mass and width of the $Y(4500)$ state are quoted from Ref. [31].

Parameter	Solution I	Solution II	Solution III	Solution IV
M_1 (MeV/c^2)	$4226.9 \pm 6.6 \pm 22.0$			
Γ_1 (MeV)	$71.7 \pm 16.2 \pm 32.8$			
$(\Gamma_{ee}\mathcal{B})_1$ (eV)	$0.13 \pm 0.02 \pm 0.05$	$0.14 \pm 0.03 \pm 0.06$	$0.18 \pm 0.05 \pm 0.07$	$0.20 \pm 0.04 \pm 0.07$
M_2 (MeV/c^2) (fixed)	$4484.7 \pm 13.3 \pm 24.1$ [Ref. [31]]			
Γ_2 (MeV) (fixed)	$111.1 \pm 30.1 \pm 15.2$ [Ref. [31]]			
$(\Gamma_{ee}\mathcal{B})_2$ (eV)	$0.08 \pm 0.09 \pm 0.04$	$0.17 \pm 0.14 \pm 0.05$	$0.31 \pm 0.26 \pm 0.11$	$0.68 \pm 0.24 \pm 0.18$
ϕ_2 (rad)	$1.02 \pm 0.57 \pm 0.56$	$1.74 \pm 1.11 \pm 0.46$	$4.26 \pm 0.76 \pm 0.91$	$4.98 \pm 0.31 \pm 0.74$
M_3 (MeV/c^2)	$4704.0 \pm 52.3 \pm 69.5$			
Γ_3 (MeV)	$183.2 \pm 114.0 \pm 96.1$			
$(\Gamma_{ee}\mathcal{B})_3$ (eV)	$0.12 \pm 0.09 \pm 0.11$	$0.68 \pm 0.26 \pm 0.21$	$0.18 \pm 0.20 \pm 0.10$	$1.04 \pm 0.60 \pm 0.35$
ϕ_3 (rad)	$0.92 \pm 0.99 \pm 0.84$	$5.37 \pm 0.46 \pm 0.95$	$5.38 \pm 1.02 \pm 0.80$	$3.55 \pm 0.27 \pm 1.03$

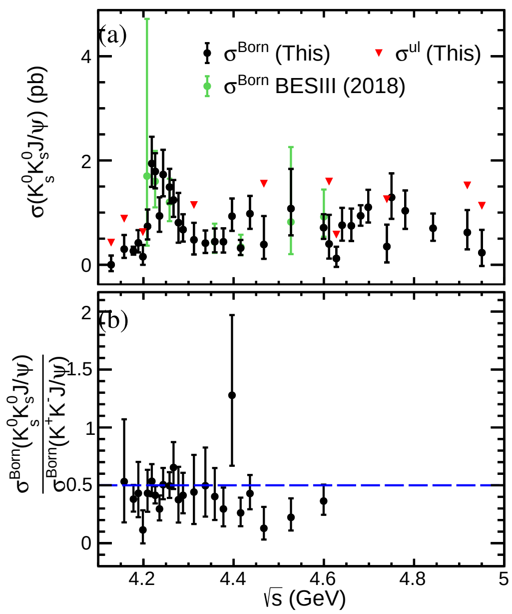

FIG. 3. (a) The Born cross sections and upper limits for $e^+e^- \to K_S^0K_S^0J/\psi$. (b) The ratio of $e^+e^- \to K_S^0K_S^0J/\psi$ to $e^+e^- \to K^+K^-J/\psi$ Born cross sections. The green and black dots with error bars in (a) are the Born cross sections from the previous measurement of the BESIII experiment [30] and this work, respectively, while the red triangles are the upper limits from this work. The blue dashed line in (b) is the value expected from isospin symmetry, and the black dots with error bars are from this study. The statistical and systematic uncertainties are included.

ucts of the electronic partial width and the branching fraction to $K_S^0K_S^0J/\psi$ $(\Gamma_{ee}\mathcal{B})_j$, and the relative phase ϕ_j between the three Breit-Wigner functions, are free. In the fit, only the statistical and uncorrelated systematic uncertainties are taken into consideration. There are four solutions for the parameters $(\Gamma_{ee}\mathcal{B})_j$ and ϕ_j as shown in Table II, and all the fit results are shown in Fig. 4.

Fitting the dressed cross sections with only two resonances ($Y(4230)$ and $Y(4710)$) yields a worse result, and the change of the likelihood value is $|\Delta(-2\ln L)| = 5.0$ compared to the three-resonance hypothesis. Taking the change in the number of degrees of freedom (2) into account, the statistical significance for the assumption of three resonant structures over the assumption of two resonant structures is 1.4σ, which indicates the $Y(4500)$ has little influence on the fits. To estimate the statistical significance of the third resonant structure, we fit the dressed cross section with the coherent sum of BW_1 and BW_2. This fit gives a worse result as well, and the change of the likelihood value is $|\Delta(-2\ln L)| = 26.3$. Taking the change in the number of degrees of freedom (4) into account, the statistical significance of the third resonant structure is 4.2σ. The significance of the third resonant structure becomes 4.0σ after taking into consideration the systematic uncertainties of the dressed cross sections.

V. SYSTEMATIC UNCERTAINTY

Systematic uncertainties in the cross section measurement mainly come from the luminosity, the branching fraction of $J/\psi \to e^+e^-/\mu^+\mu^-$, the lepton pair mass resolution, the ISR correction factor, and the detection efficiency. Systematic uncertainty from the luminosity is 0.6% based on studies of Bhabha events [34, 36, 37]. Systematic uncertainties from the subsequent branching fractions are quoted from the PDG [4]. Systematic uncertainty from the J/ψ mass window is caused by the $M(l^+l^-)$ resolution differences of data and MC simulations. To account for the differences in J/ψ mass resolution, we smear the width of the J/ψ peak in the signal MC samples, and the changes in the event selection efficiencies are less than 1.0%, which is assigned as the systematic uncertainty due to the J/ψ mass window.

To estimate the systematic uncertainty from the ISR correction factor, we compare the dressed cross sections between the last two ISR correction iterations. Due to the convergence of the iterations, the maximum difference of the dressed cross

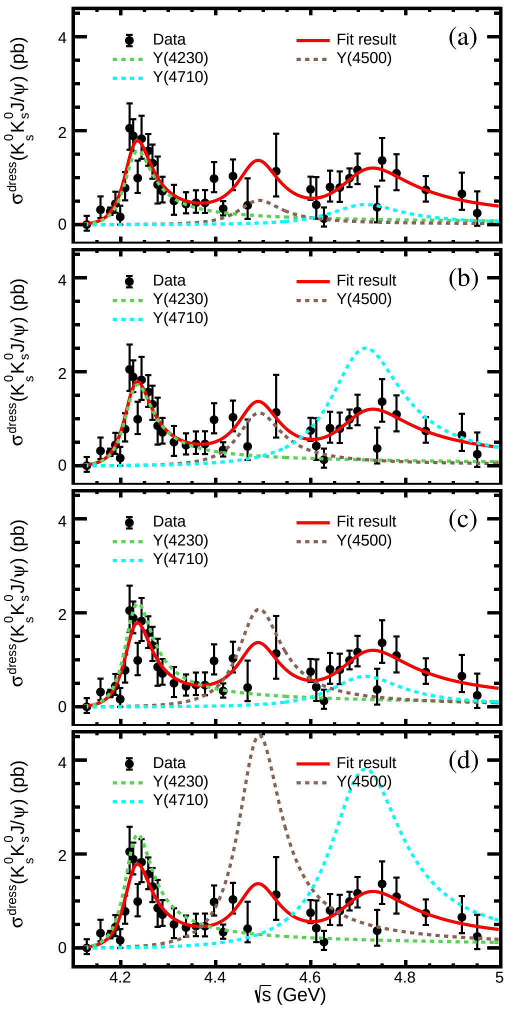

FIG. 4. Maximum likelihood fits to the dressed cross sections of $e^+e^- \to K_S^0K_S^0J/\psi$. The four solutions are shown separately in panels (a)-(d). The dots with error bars are the dressed cross sections of $e^+e^- \to K_S^0K_S^0J/\psi$; the red solid curves are the fit results using a coherent sum of three Breit-Wigner functions; and the green, brown, and the cyan dashed curves show the contributions of the $Y(4230)$, $Y(4500)$, and $Y(4710)$ states, respectively. The mass and width of the $Y(4500)$ state are fixed. The statistical and uncorrelated systematic uncertainties are included.

sections is negligible. On the other hand, in the ISR correction iterations, we also replace the description of the default dressed cross section line shape with the coherent sum of three Breit-Wigner functions and a phase-space function, or the coherent sum of two Breit-Wigner functions. In addition, we free all parameters in the coherent sum of three Breit-Wigner functions, and describe the background by a second order polynomial function. The maximum difference due to the line shape is 2.7%, which is assigned as the systematic uncertainty due to the ISR correction factor.

Sources of systematic uncertainty from the detection efficiency include systematic uncertainties in K_S^0 reconstruction (2.0% per K_S^0) [30], tracking efficiency (1.0% per track), and photon reconstruction (1.0% per photon) [55]. In addition, to account for the systematic uncertainty from the requirement on the number of photons in the four charged tracks reconstruction case, we compare the ratio of the number of events from MC simulations to data for different N_γ requirements and assign the maximum difference of 1.1% as the systematic uncertainty. The uncertainties from the two reconstruction methods are summed according to error propagation. The uncertainty due to the kinematic fit is estimated by correcting the helix parameters of the simulated charged tracks to match the resolution found in data, and changing the requirement on the χ^2 from the kinematic fit. To reduce the influence of data sample sizes, we add all the data together to estimate the differences of the ratios of signal number of events to weighted efficiency when changing the χ^2 requirement, and the maximum difference (3.7%) is assigned as the systematic uncertainty due to the kinematic fit. The systematic uncertainty due to the MC simulation model is assigned as the maximum difference between the nominal and data-weighted efficiency. Using the control sample $e^+e^- \to K^+K^-J/\psi$, we calculate the nominal efficiency directly based on the simulated exclusive MC samples. To estimate the data-weighted efficiency, we divide the invariant mass of the K^+K^- or KJ/ψ system into 10 intervals, and define the data-weighted efficiency as $\sum N_i^{\rm data}/\sum(N_i^{\rm data}w_i)$, where w_i is ϵ_i^{-1}, and $N_i^{\rm data}$ and ϵ_i are the number of signal events from data and the efficiency from signal MC in the i-th interval, respectively. We find a maximum efficiency difference of 6.8%.

TABLE III. The relative systematic uncertainties for the cross sections of the process $e^+e^- \to K_S^0K_S^0J/\psi$.

Source	Systematic uncertainty (%)
Luminosity	0.6
Branching fraction	0.4
J/ψ mass window	1.0
$(1+\delta)$	2.7
K_S^0 reconstruction	3.6
Tracking	2.0
Photon reconstruction	2.0
Kinematic fit	3.7
MC model	6.8
Sum	9.5

Assuming all sources of uncertainty are independent, the total systematic uncertainty in the $e^+e^- \to K_S^0K_S^0J/\psi$ cross section measurement is determined to be the quadratic sum of the common systematic uncertainties. The relative systematic uncertainties and their sum are shown in Table III.

The systematic uncertainties in the resonance parameters mainly come from the absolute CM energy measurement, the form and parameterization of the fit function, the CM energy spread, and the systematic uncertainty on the cross section measurement. The absolute CM energy has been measured [34–37], and the associated systematic uncertainty is estimated by varying the absolute CM energies in the fits. The uncertainty from the form of the fit function is estimated by replacing the nominal function with the coherent sum of two

TABLE IV. Systematic uncertainties in the measurement of resonance parameters, including those due to the CM energy ($\sqrt{s}$), the form of the fit function (FF), the parameterization of the fit function ($\Gamma_{\rm tot}$), the CM energy spread (ES), and the uncorrelated ($\sigma_1^{\rm dress}$) and correlated ($\sigma_2^{\rm dress}$) systematic uncertainties from the cross section measurements. The symbol "–" represents negligible uncertainties.

Parameter	$\sqrt{s}$	FF	$\Gamma_{\rm tot}$	ES	$\sigma_1^{\rm dress}$	$\sigma_2^{\rm dress}$	Sum
M_1 (MeV/c^2)	0.9	2.2	21.9	0.1	0.1	–	22.0
M_3 (MeV/c^2)	1.2	5.3	69.3	0.3	0.2	–	69.5
Γ_1 (MeV)	0.5	9.5	31.4	0.2	0.7	–	32.8
Γ_3 (MeV)	0.8	33.9	89.9	0.4	0.2	–	96.1
$(\Gamma_{ee}\mathcal{B})_1$ (eV)	–	0.02	0.05	–	–	0.01	0.05
	–	0.02	0.06	–	–	0.01	0.06
	–	0.03	0.06	–	–	0.01	0.07
	–	0.03	0.06	–	–	0.01	0.07
$(\Gamma_{ee}\mathcal{B})_2$ (eV)	–	0.02	0.03	–	–	–	0.04
	–	0.03	0.04	–	–	0.01	0.05
	–	0.07	0.08	–	–	0.02	0.11
	–	0.13	0.12	–	–	0.04	0.18
$(\Gamma_{ee}\mathcal{B})_3$ (eV)	–	0.03	0.11	–	–	0.01	0.11
	–	0.21	0.01	–	–	0.04	0.21
	–	0.06	0.08	–	–	0.01	0.10
	–	0.34	0.06	–	–	0.06	0.35
ϕ_2 (rad)	–	0.34	0.44	0.01	0.01	0.06	0.56
	–	0.42	0.15	0.01	0.01	0.10	0.46
	–	0.40	0.78	–	–	0.26	0.91
	–	0.34	0.58	–	–	0.30	0.74
ϕ_3 (rad)	–	0.84	0.05	–	–	0.06	0.84
	–	0.65	0.61	0.01	0.01	0.32	0.95
	–	0.70	0.21	0.01	0.01	0.32	0.80
	–	0.73	0.70	–	–	0.21	1.03

Breit-Wigner functions, or the coherent sum of three Breit-Wigner functions and a phase-space function. To estimate the uncertainty from the form of the Breit-Wigner function, the Γ_j in the denominator of the Breit-Wigner function is replaced with a mass-dependent width $\Gamma_j \frac{\Phi(\sqrt{s})}{\Phi(M_j)}$. The uncertainty from the CM energy spread is estimated by convolving the fit formula with a Gaussian function, whose width is set as the mass-dependent beam spread [56]. The uncertainty from the cross section measurement is divided into two parts. The first one is uncorrelated uncertainties of the cross sections among the different CM energy points, and comes mainly from the fit to the $M(l^+l^-)$ spectrum to determine the signal yields. The corresponding uncertainty is estimated by including the uncorrelated uncertainties in the dressed cross section fits, and the differences on the parameters are taken as the corresponding uncertainties. The second part, including all other uncertainties of the cross sections, is common for all data points (6.0%), and only affects the parameter $(\Gamma_{ee}\mathcal{B})$. The systematic uncertainties in the resonance parameters are shown in Table IV.

VI. SUMMARY

In summary, we measure the Born cross sections of the process $e^+e^- \to K_S^0 K_S^0 J/\psi$ at CM energies from 4.128 to 4.950 GeV. The measured Born cross sections are consistent with the previous measurements of the BESIII experiment [30], as shown in Fig. 3.

A clear resonant structure for the $Y(4230)$ is observed via $e^+e^- \to K_S^0 K_S^0 J/\psi$ for the first time, and the mass and width of the $Y(4230)$ are determined to be $M(Y(4230)) = 4226.9 \pm 6.6 \pm 22.0$ MeV/c^2 and $\Gamma(Y(4230)) = 71.7 \pm 16.2 \pm 32.8$ MeV, where the first uncertainties are statistical and the second are systematic. In addition, we see another enhanced structure with a statistical significance 4.2σ, called the $Y(4710)$. The mass and width of the $Y(4710)$ are determined to be $M(Y(4710)) = 4704.0 \pm 52.3 \pm 69.5$ MeV/c^2 and $\Gamma(Y(4710)) = 183.2 \pm 114.0 \pm 96.1$ MeV, respectively. If this structure is the $\psi(5S)$, the measured mass will be in favor of the linear potential model predictions [57]. It is also in agreement with the results based on the BaBar experiment [58–60].

The average Born cross section ratio $\frac{\sigma^{\rm Born}(K_S^0 K_S^0 J/\psi)}{\sigma^{\rm Born}(K^+K^- J/\psi)}$ is determined to be $0.388^{+0.035}_{-0.028} \pm 0.016$ based on an asymmetric Gaussian fit of combined ratio likelihood simulations, where the statistical uncertainty is obtained by the fit, and the common items of the systematic uncertainties have been canceled. The P-value of the ratio likelihood distribution greater than 0.5 is 0.0011 which indicates a 3.1σ significance isospin violation effect in $e^+e^- \to K\bar{K}J/\psi$. When taking the three-body phase space into consideration, the average Born cross section ratio becomes $0.426^{+0.038}_{-0.031} \pm 0.018$, with a P-value of 0.0304, which indicates an isospin violation effect in $e^+e^- \to K\bar{K}J/\psi$ with 1.9σ significance.

Using the measured products of the electronic partial width and the decay branching fractions $\Gamma(e^+e^- \to Y(4230))\mathcal{B}(Y(4230) \to K_S^0 K_S^0 J/\psi)$ (Table II) and $\Gamma(e^+e^- \to Y(4230))\mathcal{B}(Y(4230) \to K^+K^- J/\psi)$ [31], the branching fraction ratio of $Y(4230) \to K_S^0 K_S^0 J/\psi$ to $Y(4230) \to K^+K^- J/\psi$ is determined to be $0.3 < \frac{\mathcal{B}(Y(4230)\to K_S^0 K_S^0 J/\psi)}{\mathcal{B}(Y(4230)\to K^+K^- J/\psi)} < 0.7$, where the large range of values is due to multiple fit solutions. It is hard to make a clear conclusion about the consistency of the experimental measurements with the theoretically expected value of 0.5 assuming the events are all from an isospin zero initial state.

We do not see a significant $Y(4500)$ contribution in the measured cross sections of $e^+e^- \to K_S^0 K_S^0 J/\psi$ due to a lack of data samples around 4.500 GeV. The maximum likelihood fit gives a statistical significance of the $Y(4500)$ of less than 1.4σ. Larger data samples are required to draw clear conclusions about the existence of the $Y(4500)$ and $Y(4710)$ states.

VII. ACKNOWLEDGEMENTS

The BESIII collaboration thanks the staff of BEPCII and the IHEP computing center for their strong support. This work is supported in part by National Key R&D

Program of China under Contracts Nos. 2020YFA0406300, 2020YFA0406400; National Natural Science Foundation of China (NSFC) under Contracts Nos. 11635010, 11735014, 11835012, 11935015, 11935016, 11935018, 11961141012, 12022510, 12025502, 12035009, 12035013, 12192260, 12192261, 12192262, 12192263, 12192264, 12192265; the Chinese Academy of Sciences (CAS) Large-Scale Scientific Facility Program; Joint Large-Scale Scientific Facility Funds of the NSFC and CAS under Contract No. U1832207; 100 Talents Program of CAS; The Institute of Nuclear and Particle Physics (INPAC) and Shanghai Key Laboratory for Particle Physics and Cosmology; ERC under Contract No. 758462; European Union's Horizon 2020 research and innovation programme under Marie Sklodowska-Curie grant agreement under Contract No. 894790; German Research Foundation DFG under Contracts Nos. 443159800, Collaborative Research Center CRC 1044, GRK 2149; Istituto Nazionale di Fisica Nucleare, Italy; Ministry of Development of Turkey under Contract No. DPT2006K-120470; National Science and Technology fund; National Science Research and Innovation Fund (NSRF) via the Program Management Unit for Human Resources & Institutional Development, Research and Innovation under Contract No. B16F640076; STFC (United Kingdom); Suranaree University of Technology (SUT), Thailand Science Research and Innovation (TSRI), and National Science Research and Innovation Fund (NSRF) under Contract No. 160355; The Royal Society, UK under Contracts Nos. DH140054, DH160214; The Swedish Research Council; U. S. Department of Energy under Contract No. DE-FG02-05ER41374.

---

[1] T. Barnes, S. Godfrey, and E. S. Swanson, Phys. Rev. D **72**, 054026 (2005).
[2] N. Brambilla *et al.*, Eur. Phys. J. C **71**, 1534 (2011).
[3] R. A. Briceno *et al.*, Chin. Phys. C **40**, 042001 (2016).
[4] R. L. Workman *et al.* (Particle Data Group), PTEP **2022**, 083C01 (2022).
[5] B. Aubert *et al.* (BaBar Collaboration), Phys. Rev. D **76**, 111105 (2007).
[6] G. Pakhlova *et al.* (Belle Collaboration), Phys. Rev. D **77**, 011103 (2008).
[7] B. Aubert *et al.* (BaBar Collaboration), Phys. Rev. Lett. **95**, 142001 (2005).
[8] T. E. Coan *et al.* (CLEO Collaboration), Phys. Rev. Lett. **96**, 162003 (2006).
[9] C. Z. Yuan *et al.* (Belle Collaboration), Phys. Rev. Lett. **99**, 182004 (2007).
[10] L. Maiani, V. Riquer, F. Piccinini, and A. D. Polosa, Phys. Rev. D **72**, 031502 (2005).
[11] G. J. Ding, Phys. Rev. D **79**, 014001 (2009).
[12] Q. Wang, C. Hanhart, and Q. Zhao, Phys. Rev. Lett. **111**, 132003 (2013).
[13] M. Alberti, G. S. Bali, S. Collins, F. Knechtli, G. Moir, and W. Söldner, Phys. Rev. D **95**, 074501 (2017).
[14] X. Li and M. B. Voloshin, Mod. Phys. Lett. A **29**, 1450060 (2014).
[15] S. L. Zhu, Phys. Lett. B **625**, 212 (2005).
[16] F. E. Close and P. R. Page, Phys. Lett. B **628**, 215 (2005).
[17] E. Kou and O. Pene, Phys. Lett. B **631**, 164 (2005).
[18] F. K. Guo, C. Hidalgo-Duque, J. Nieves, and M. P. Valderrama, Phys. Rev. D **88**, 054007 (2013).
[19] L. Maiani, V. Riquer, R. Faccini, F. Piccinini, A. Pilloni, and A. D. Polosa, Phys. Rev. D **87**, 111102 (2013).
[20] E. Braaten, Phys. Rev. Lett. **111**, 162003 (2013).
[21] X. H. Liu and G. Li, Phys. Rev. D **88**, 014013 (2013).
[22] M. Ablikim *et al.* (BESIII Collaboration), Phys. Rev. Lett. **118**, 092001 (2017).
[23] M. Ablikim (BESIII Collaboration), Phys. Rev. D **102**, 012009 (2020).
[24] M. Ablikim *et al.* (BESIII Collaboration), Phys. Rev. Lett. **118**, 092002 (2017).
[25] M. Ablikim *et al.* (BESIII Collaboration), Phys. Rev. D **96**, 032004 (2017), [Erratum: Phys.Rev.D 99, 019903 (2019)].
[26] M. Ablikim *et al.* (BESIII Collaboration), Phys. Rev. D **97**, 052001 (2018).
[27] M. Ablikim *et al.* (BESIII Collaboration), Phys. Rev. D **104**, 052012 (2021).
[28] M. Ablikim *et al.* (BESIII Collaboration), Phys. Rev. Lett. **114**, 092003 (2015).
[29] M. Ablikim *et al.* (BESIII Collaboration), Phys. Rev. D **99**, 091103 (2019).
[30] M. Ablikim *et al.* (BESIII Collaboration), Phys. Rev. D **97**, 071101 (2018).
[31] M. Ablikim *et al.* ((BESIII),, BESIII), Chin. Phys. C **46**, 111002 (2022).
[32] C. Z. Yuan *et al.* (Belle Collaboration), Phys. Rev. D **77**, 011105 (2008).
[33] C. P. Shen *et al.* (Belle Collaboration), Phys. Rev. D **89**, 072015 (2014).
[34] M. Ablikim *et al.* (BESIII Collaboration), Chin. Phys. C **39**, 093001 (2015).
[35] M. Ablikim *et al.* (BESIII Collaboration), Chin. Phys. C **45**, 103001 (2021).
[36] M. Ablikim *et al.* (BESIII Collaboration), (2022), arXiv:2203.03133 [hep-ex].
[37] M. Ablikim *et al.* (BESIII Collaboration), (2022), arXiv:2205.04809 [hep-ex].
[38] M. Ablikim *et al.* (BESIII Collaboration), Nucl. Instrum. Meth. A **614**, 345 (2010).
[39] C. Yu *et al.*, in *7th International Particle Accelerator Conference* (2016) p. TUYA01.
[40] M. Ablikim *et al.* (BESIII Collaboration), Chin. Phys. C **44**, 040001 (2020).
[41] K.-X. Huang, Z.-J. Li, Z. Qian, J. Zhu, H.-Y. Li, Y.-M. Zhang, S.-S. Sun, and Z.-Y. You, Nucl. Sci. Tech. **33**, 142 (2022).
[42] P. Cao *et al.*, Nucl. Instrum. Meth. A **953**, 163053 (2020).
[43] S. Agostinelli *et al.* (GEANT4 Collaboration), Nucl. Instrum. Meth. A **506**, 250 (2003).
[44] S. Jadach, B. F. L. Ward, and Z. Was, Comput. Phys. Commun. **130**, 260 (2000).
[45] S. Jadach, B. F. L. Ward, and Z. Was, Phys. Rev. D **63**, 113009 (2001).
[46] D. J. Lange, Nucl. Instrum. Meth. A **462**, 152 (2001).
[47] R. G. Ping, Chin. Phys. C **32**, 599 (2008).
[48] J. C. Chen, G. S. Huang, X. R. Qi, D. H. Zhang, and Y. S. Zhu, Phys. Rev. D **62**, 034003 (2000).

[49] R. L. Yang, R. G. Ping, and H. Chen, Chin. Phys. Lett. **31**, 061301 (2014).
[50] E. Richter-Was, Phys. Lett. B **303**, 163 (1993).
[51] R. G. Ping, Chin. Phys. C **38**, 083001 (2014).
[52] W. Sun, T. Liu, M. Jing, L. Wang, B. Zhong, and W. Song, Front. Phys. (Beijing) **16**, 64501 (2021).
[53] S. Actis *et al.* (Working Group on Radiative Corrections, Monte Carlo Generators for Low Energies), Eur. Phys. J. C **66**, 585 (2010).
[54] W. A. Rolke, A. M. Lopez, and J. Conrad, Nucl. Instrum. Meth. A **551**, 493 (2005).
[55] M. Ablikim *et al.* (BESIII Collaboration), Phys. Rev. D **91**, 112005 (2015).
[56] E. V. Abakumova *et al.*, Nucl. Instrum. Meth. A **659**, 21 (2011).
[57] L. C. Gui, L. S. Lu, Q. F. Lü, X. H. Zhong, and Q. Zhao, Phys. Rev. D **98**, 016010 (2018).
[58] E. van Beveren and G. Rupp, Chin. Phys. C **35**, 319 (2011).
[59] E. van Beveren and G. Rupp, (2009), arXiv:0904.4351 [hep-ph].
[60] E. van Beveren, X. Liu, R. Coimbra, and G. Rupp, EPL **85**, 61002 (2009).